Theoretical treatment of analog (p,n) cross sections for odd nuclei: Application to measurements of ^{105}Pd at 26 MeV

V. A. Madsen,* R. W. Bauer, J. D. Anderson, V. R. Brown, B. A. Pohl, and C. H. Poppe
Lawrence Livermore National Laboratory, University of California, Livermore, California 94550

S. Stamer, E. Mordhorst, and W. Scobel
I. Institut für Experimentalphysik, University of Hamburg, Hamburg, Federal Republic of Germany

S. M. Grimes
Ohio University, Athens, Ohio 45701

(Received 1 October 1992)

Differential cross sections for the (p,n) reaction to the ground-state and excited-state analogs of ^{105}Pd have been measured at a proton bombarding energy of 26 MeV. Both the magnitude and the angular distribution of the cross sections for the analog states are found to follow the same general trend observed for the even-even palladium isotopes. Contributions to the analog transition on odd-A targets from spin-flip, higher multipoles, collective admixtures, and multistep processes are calculated and are found to be of order $1/(N-Z)$ or smaller, as compared to the $(N-Z)$ scaling expected for the Fermi transition. This is in agreement with our experimental data which show that the analog cross section scales as $(N-Z)$ relative to the neighboring nuclei. Among the excited analog states within the first MeV of excitation, the levels at 0.44 and 0.78 MeV were the most strongly populated. This is consistent with a two-step mechanism involving inelastic scattering and charge exchange, since these two states are also known to have the largest $B(E2)$ values. Although the small predicted magnitude of the additional contributions for nonzero spin targets agrees nicely with the present measurements for ^{105}Pd, it leaves the puzzle as to why cross sections for odd isotopes for titanium and molybdenum measured in previous work were found to be larger than corresponding cross sections for adjacent even isotopes.

PACS number(s): 25.40.Kv, 21.10.Hw, 27.60.+j

I. INTRODUCTION

This paper reports measurements of the differential cross sections for the (p,n) reaction to the ground- and excited-state analogs of ^{105}Pd. This work is a continuation of our experimental program to investigate isobaric analog states in the nuclear mass region near $A=100$. Our previously reported analog cross sections (see, e.g., Refs. [1–3]) have demonstrated a considerable departure from the Lane-model prediction [4] of near proportionality to $(N-Z)$. Coupled-channels calculations [1] indicated that this deviation can be explained by couplings to the low-lying collective states and their analogs. The deviation can be explained in terms of three 3-step amplitudes, all nearly in phase, each involving two collective inelastic transitions and one charge-exchange transition. These calculations confirmed that the excitation of analogs of strong collective states proceeds primarily by two-step mechanisms, the effect of the one-step process being negligibly small in most cases [1]. The variation of $\sigma/(N-Z)$ from constancy was expected to be greatest for nuclei with large deformation parameters. This was demonstrated for the even-even isotopes of molybdenum, zirconium, and palladium [1–3]. This effect has been clearly explained by the coupled-channels model.

One aspect of the earlier studies which was not explained was the apparent enhancement [5–8] of some (^{47}Ti, ^{49}Ti, ^{95}Mo) analog cross sections relative to the neighboring even isotopes, while other odd isotopes (^{91}Zr, ^{97}Mo) showed behavior consistent with adjacent even isotopes. An obvious possibility is that higher multipoles contribute to the cross sections. An even-even target has ground state and analog spin zero, allowing only monopole contributions, but the isotopes with $J\neq 0$ could in principle have multipoles up to order $2J$ contributing to the cross sections. An attempt to explain the cross sections as due to spin flip for the odd titanium isotopes [9,10] gave non-negligible effects, but did not yield contributions as large as needed to match the experimental values. The purpose of the present study was to broaden the database on odd-even differences in analog states by measuring cross sections for ^{105}Pd to compare with adjacent even isotopes [3]. At the same time, a careful examination of theoretical predictions is presented not just for spin flip, but also higher multipoles, collective admixtures in the ground state, and higher-order (multistep) contributions to the analog cross section.

Section II of this paper gives a description of our experiment and the methods used for data reduction. Section III contains the theoretical development, Sec. IV is a discussion of our results, and Sec. V presents a summary and our conclusions.

*Permanent address: Oregon State University, Corvallis, OR 97331.

II. EXPERIMENTAL METHOD AND DATA REDUCTION

The experiment was carried out in two separate runs at the Hamburg Isochronous Cyclotron Facility. The energy of the incident proton beam was 25.9±0.1 MeV in the first series of measurements, 26.1±0.1 MeV in the second series. The beam impinged on a self-supporting target foil of highly enriched (>93%) palladium (^{105}Pd) with a thickness of 5.0 mg/cm^2. A beam burst separation of 829 ns was obtained by effectively (>99.8%) suppressing 15 out of 16 bursts with an external deflection system. The resulting beam intensity of approximately 80 nA allowed one set of measurements to be completed within 4 h with a charge of typically 1 mC accumulated in the heavily shielded Faraday cup. A schematic layout of the beam line together with the target chamber and the neutron time-of-flight setup is shown in Ref. [3].

The standard Hamburg neutron time-of-flight (TOF) setup, consisting of eight detectors and three possible target positions, covers an angular range of $3° \leq \theta_{lab} \leq 177°$ with 24 roughly equidistant positions. Details of this experimental setup and its performance in neutron spectroscopy have been described previously [11,12]. For the present experiment, this setup was modified to improve the neutron resolution for the angles $\theta_{lab} \leq 60°$. Details of the modifications as well as the characteristics of the time-of-flight detectors used in this experiment have been presented in Ref. [3]. With these improvements effective n-γ pulse-shape discrimination was obtained and an overall neutron energy resolution ranging from 125 to 200 keV, depending on the individual detectors, was achieved for the isobaric analog transitions ($E_n \approx 12.5$ MeV).

A representative TOF spectrum for a detector at the flight path of approximately 20 m is shown in Fig. 2 of Ref. [3]. The conversation into absolute energy spectra, achieved by using time calibrations derived from the positions of the (strongly reduced) gamma peaks from two subsequent beam bursts, and the detector efficiency calculations have been described previously [3]. The uncertainties resulting from target inhomogeneities and impurities (<5%), incomplete beam current integration (<3%), and detector efficiency (≤4%) lead to a minimum uncertainty $\Delta\sigma/\sigma = 7\%$ of the differential cross sections. Additional contributions to the uncertainty are due to counting statistics and peak integration (see below).

The characteristic features of the neutron TOF spectra, as seen in Fig. 1, are a number of neutron peaks superimposed on the neutron continuum. The $\frac{5}{2}^+$ ground state is clearly identifiable in the spectra for all the 24 angles measured. Kinematic calculations were used to locate the low-lying excited analog states, two of which were discernable in all but some of the backward angles. In order to determine the counts of the respective peaks, the peak-fitting program FITEK was used [13]. This program is highly interactive and is used to fit the peaks as well as the background underneath them. During the first pass, when fitting the major features of the spectrum, in addition to the ground-state analog peak only two secondary

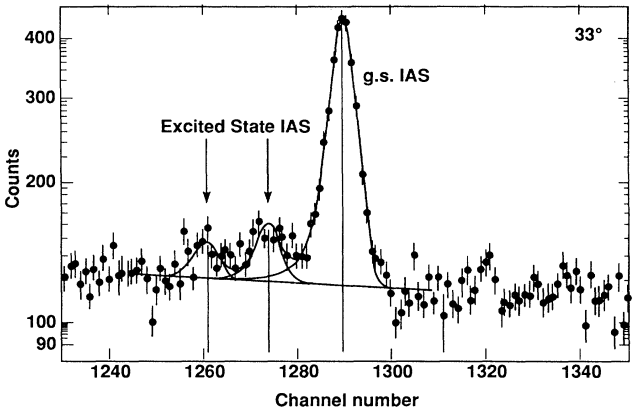

FIG. 1. Representative TOF spectrum of the ground-state analog peak and two excited-state analog peaks for the ^{106}Pd$(p,n)^{105}$Ag reaction at 26 MeV proton energy. The solid curve through the data points is an example of the fit generated by the FITEK program. Note that the ordinate is a logarithmic scale, while the abscissa is linear in channels and increasing time is toward the left.

peaks were found which corresponded to excited-state analogs with excitation energies of approximately 0.44 and 0.78 MeV. These energies were known to correspond to the excited states in ^{105}Pd with the largest $B(E2)$ values obtained in Coulomb excitation [14,15] as seen in Table I. No measurable signals were observed for the other known excited states (within the first MeV of excitation). Thus the energy values of the two dominant excited-state peaks were adopted in the subsequent pass of the fitting procedure. In this analysis, kinematics were used to fix the positions of the two minor peaks, i.e., the excited-state analogs at 0.44 and 0.78 MeV, with respect to the major peak, i.e., the ground-state analog. An example of a FITEK result is given in Fig. 1. The peak shape for the ground-state analog was found to be a skewed Gaussian with a small tail toward higher excita-

TABLE I. Levels in ^{105}Pd observed by Coulomb excitation by Bolotin and McClure [14]. [$B(E2)$ values in parentheses are additional values listed in the compilation by De Frenne *et al.* [15]].

Energy of excitation (MeV)	Spin and parity	$10^{-4}B(E2)$
0 (ground state)	$\frac{5}{2}^+$	
0.280	$\frac{3}{2}^+$	110±10(20±10)
0.306	$\frac{7}{2}^+$	12±2(40±10)
0.319	$\frac{5}{2}^+$	81±10(80±20)
0.344	$\frac{1}{2}^+$	15±3(28±3)
0.442	$(\frac{7}{2}^+)$	1650±130(1800±400)
0.561	$\frac{5}{2}^+$	75±10(60±20)
0.651	$\frac{3}{2}^+$	66±13(170±50)
0.673	$\frac{1}{2}^+$	57±11(50±30)
0.727	$\frac{5}{2}^+$	24±6(100±30)
0.782	$\frac{9}{2}^+$	827±83(1200±100)

tion. This same shape was also imposed on the excited-state analogs during the final FITEK analysis. The integral under the curve determined the sum of the counts in the respective peak. The uncertainty, as determined by FITEK, includes the statistical error of the signal and background as well as the error due to the deviation of the individual data points from the skewed Gaussian defined by the FITEK program. Thus the total calculated error includes both the statistics and a measure of the goodness of the fit of the Gaussian to the data. This total error was combined with the systematic uncertainty of 7% discussed above.

Using the counts in the respective peaks, together with the previously determined detector efficiencies and known target thickness, we calculated the differential cross sections for the ground-state analog peak ($\frac{5}{2}^+$), for the excited state at 0.44 MeV ($\frac{7}{2}^+$), and for the excited state at 0.78 MeV ($\frac{9}{2}^+$). For the other excited states (within the first MeV of excitation), the cross sections were found to be below the limit of our detectability; they are estimated to be at least one order of magnitude less than those for the 0.78 MeV excited state. Figure 2 shows the differential cross sections to the three states which had measurable cross sections.

Each of the three measured angular distributions was fitted with a series of Legendre polynomials in order to determine the integrated cross section. Errors in the integrated cross sections were determined both from the relative errors in the individual data points and from the goodness of fit of the polynomial series of the data. The results are presented in Table II.

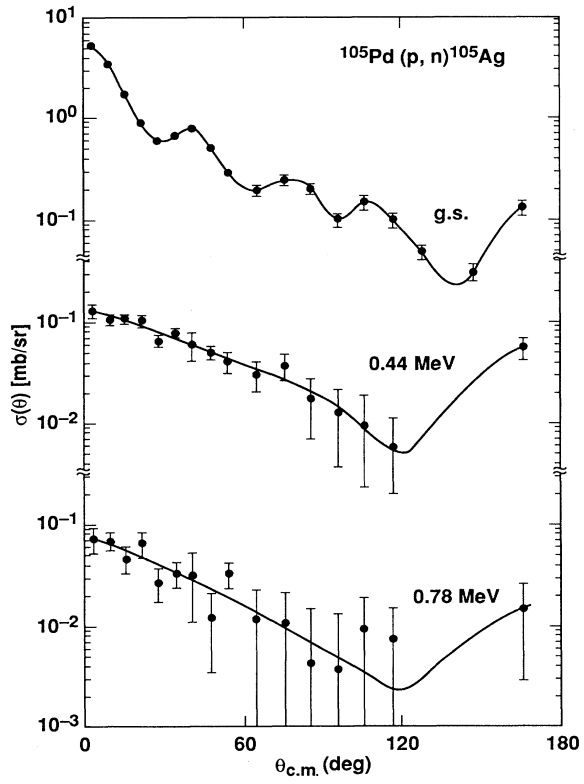

FIG. 2. Angular distribution for the ^{105}Pd$(p,n)^{105}$Ag reaction to the ground-state analog and two excited-state analogs. The absolute cross sections are shown. The solid curves are provided as a guide to the eye.

TABLE II. Integrated ^{105}Pd(p,n) cross sections to the ground-state analog and two excited-state analogs at a bombarding energy of 26 MeV.

Energy of excitation of analog state (MeV)	Spin and parity	σ (experimental results) (mb)
0 (ground state)	$\frac{5}{2}^+$	3.75±0.27
0.44	$(\frac{7}{2}^+)$	0.40±0.035
0.78	$(\frac{9}{2}^+)$	0.18±0.06

III. THEORY

A. Introductory remarks

The contribution to analog states of odd-A nuclei has been treated for the Gamow-Teller operator [9,10] for spin-flip transitions in the odd isotopes of titanium by using MBZ (McCullen-Bayman-Zamick) purely $f_{\frac{7}{2}}$ configuration wave functions [16]. The result was that, whereas for Fermi-like excitations (total angular momentum transfer $=0$) of analog states the cross section is proportional to $(N-Z)$, the spin-flip transitions go as $1/(N-Z)$. Thus only for nuclei with a very small neutron excess would spin-flip amplitudes contribute significantly to the cross section.

The same dependence on $(N-Z)$ holds for a transition operator of any other multipolarity. The physical reason for this effect is that ground states of odd nuclei consist mostly of nucleons coupled to zero in pairs; the spectroscopic properties are then determined by the one unpaired nucleon, as in the Schmidt model [17]. In the seniority framework [18], this property is described by saying that an odd-A nucleus is dominated by seniority 1 (only one unpaired nucleon) and that components of the wave function with higher seniority are fairly small. Operators of multiplicity $I>0$ operate primarily on the last unpaired nucleon. The presence of the paired nucleons gives a transition amplitude less than or equal to that for a pure single-particle transition because of exclusion principle effects.

In Sec. III B the charge-exchange matrix element is converted into an isovector elastic scattering matrix element. The matrix element for the $I\equiv|\Delta\mathbf{J}|=0$ multipole is then expressed in terms of number operators. In Sec. III C and Appendix A, the analog matrix elements for higher multipolarities are estimated on the basis of the seniority model. Appendix B contains a derivation of the nucleon pair commutation relations and normalization constants for seniority wave functions. Section III D and Appendix C contain a derivation of estimates of the effects of virtual collective states induced in the even-even core by the unpaired odd particle. These are made by relating the charge-exchange matrix element to collective

inelastic scattering cross sections in the neighboring even-A nuclei. In Sec. III E the possible effects of multistep processes, known to be important for analog transitions, are examined on the basis of the collective particle-core coupling model.

B. Analog matrix elements

Assuming the conservation of isospin, the transition matrix element between analog states in a charge-exchange reaction can be written in terms of the elastic transition

$$\langle JMT,T-1|V|JMTT\rangle = (2T)^{-1/2}\langle JMTT|[\mathbf{T}_+,V]|JMTT\rangle \ . \quad (1)$$

The central-tensor interaction V between projectile, labeled 0, and target particle, labeled 1, is

$$V=\sum_{ISL\lambda\tau N\rho}[(-1)^{N+\rho}\mathcal{Y}_{I(LS),-N}(0)\mathcal{Y}_{I(\lambda S)N}(1)\mathcal{T}_{\tau,-\rho}(0)\mathcal{T}_{\tau\rho}(1)](-1)^{I-S-L}F_{I(LS)\lambda\tau\rho}(r_0,r_i) \ , \quad (2)$$

where

$$\mathcal{Y}_{I(\lambda S)N}(1)=[Y_l(\hat{r}_i)\mathcal{S}_S(1)]_{I(\lambda S)N} \ , \quad (3)$$

$$\mathcal{S}_{S\mu}=\begin{cases}\sigma_\mu, & S=1\\ 1, & S=0\end{cases} \ , \quad (4a)$$

$$\mathcal{T}_{\tau\rho}=\begin{cases}\tau_\rho, & \tau=1\\ 1, & \tau=0\end{cases} \ , \quad (4b)$$

and F is a radial function. Our argument involves only the operator on the nuclear coordinate. For conciseness and to emphasize that the following development applies to any nuclear one-body, charge-exchange multipole operator, we substitute a generic one-body operator

$$\sum_{i=1}^{A}\mathcal{Y}_{I(\lambda S)N}(i)\mathcal{T}_{\tau\rho}(i)F_{I(\lambda S)\tau}(r_i)\rightarrow\sum_i \mathbf{Q}_{IN}(i)\mathcal{T}_{\tau\rho}(i) \ , \quad (5)$$

where I, λ, and S, are, respectively, the total, orbital, and spin angular momentum transfers to the nucleus, $N=I_z$, τ is the isospin transfer, and $\rho=\tau_z$ is -1 for a (p,n)-like charge-exchange transition.

The essential part of the operator commutation relation in Eq. (1) is therefore

$$[\mathbf{T}_+,\tau_{-1}(1)]=2^{-1/2}[\tau_+(1),\tau_-(1)]=2^{+1/2}\tau_z(1) \ . \quad (6)$$

The charge-exchange matrix element, Eq. (1), may then be rewritten as an elastic matrix element of an isovector operator

$$\left\langle JMT,T-1\left|\sum_i \mathbf{Q}_{IN}(i)\tau_{-1}(i)\right|JMTT\right\rangle = \left[\frac{2}{N-Z}\right]^{1/2}\left\langle JMTT\left|\sum_i \mathbf{Q}_{IN}(i)\tau_z(i)\right|JMTT\right\rangle \ . \quad (7)$$

In second quantized notation, the operator in Eq. (7) is

$$\left[\frac{2}{N-Z}\right]^{1/2}\sum_{j_1m_1j_2m_2}\langle j_2m_2\alpha|Q_{IN}(1)\tau_z(1)|j_1m_1\alpha\rangle a^\dagger_{j_2m_2\alpha}a_{j_1m_1\alpha} = \left[\frac{2}{N-Z}\right]^{1/2}\frac{1}{\hat{I}}\sum_{j_1j_2\alpha}(-1)^{j_1-j_2+I}(2\alpha)\langle j_2\alpha\|Q_I\|j_1\alpha\rangle[a^\dagger_{j_2\alpha}\tilde{a}_{j_1\alpha}]_{IN} \ , \quad (8)$$

where $\tilde{a}_{jm}$ is the irreducible tensor operator

$$\tilde{a}_{jm}=(1)^{j-m}a_{j,-m} \quad (9)$$

and the brackets denote coupling of the operators. The isospin factor 2α is ±1 for the neutrons and protons, respectively. The single-particle reduced matrix element depends on the nucleon isospin only through the single neutron or proton radial integral. For simplicity, we assume that the operator Q_{IN} separates, as in Eq. (2), into a product of a radial function and a spin spherical harmonic [see Eq. (3)],

$$Q_{IN}=g(r)\mathcal{Y}_{I(\lambda S)N} \ . \quad (10)$$

Then we may write

$$[a^\dagger_{j_2\alpha}\tilde{a}_{j_1\alpha}]_{00}=\sum_{m_1m_2}\langle j_1j_2m_1m_2|00\rangle a^\dagger_{j_2m_2\alpha}a_{j_1m_1\alpha} = \frac{\delta j_1j_1}{\hat{j}_1}\sum_m a^\dagger_{j_1m\alpha}a_{j_1m\alpha} = \frac{\delta j_1j_2}{\hat{j}_1}\mathcal{N}_{j_1\alpha} \ , \quad (11)$$

where $\mathcal{N}_{j_1\alpha}$ is the j-level number operator for nucleons of type α. Since

$$\langle j_1m_1\alpha|\mathbf{Q}_{00}|j_1m_1\alpha\rangle = \int\psi^\dagger_{j_1m_1\alpha}(r)g(r)(4\pi)^{-1/2}\psi_{j_1m_1\alpha}(r)d^3r = (4\pi)^{-1/2}\int|R_{j_1\alpha}(r)|^2g(r)r^2dr = (4\pi)^{-1/2}\rho_{j_1\alpha} \ , \quad (12)$$

where $\rho_{j_1\alpha}$ is the radial integral, the matrix element, Eq. (7), for $I=N=0$ is

$$\left\langle JMT,T-1\left|\sum_i \mathbf{Q}_{00}(i)\tau_{-1}(i)\right|JMTT\right\rangle=(4\pi)^{-1/2}\left[\frac{2}{N-Z}\right]^{1/2}\sum_{j\alpha}\rho_{j\alpha}\langle JMTT|\mathcal{N}_{j\alpha}|JMTT\rangle$$
$$=\left[\frac{2}{N-Z}\right]^{1/2}\sum_j(\rho_{j,1/2}\mathcal{N}_{j,1/2}-\rho_{j,-1/2}\mathcal{N}_{j,-1/2})\ . \tag{13}$$

To the extent that isospin is exact (neutron and proton orbitals the same), this is

$$\left[\frac{1}{2(N-Z)}\right]^{1/2}\left[\mathbf{T}_+,\sum_i \mathbf{Q}_{00}(i)\tau_{-1}(i)\right]=(4\pi)^{-1/2}\left[\frac{2}{N-Z}\right]^{1/2}\sum_j\rho_j(\mathcal{N}_{j,1/2}-\mathcal{N}_{j,-1/2})\ . \tag{14}$$

Furthermore, to a fair approximation [exact for the allowed Fermi operator $g(r)=1$], $\rho_{j,1/2}$ is independent of j, which gives

$$\left\langle JMT,T-1\left|\sum_i \mathbf{Q}_{00}(i)\tau_{-1}(i)\right|JMTT\right\rangle=(4\pi)^{-1/2}[2(N-Z)]^{1/2}\rho_{j,1/2}\ . \tag{15}$$

The rate or cross section for a charge-exchange process is then proportional to the squared matrix element, i.e., the rate $\sim(N-Z)$, the well-known (approximate) dependence on neutron excess.

For odd nuclei, multipoles other than $I=0$, up to $2J$, may occur. These are nearly incoherent with each other, and so they each add a positive contribution to the cross section. We show in the following development that higher multipoles and contributions to the cross section vary approximately as $(N-Z)^{-1}$, that is, as $(N-Z)^{-2}$ times the Fermi rate. These numerical factors bring the possible $I>0$ contribution for the odd Ti isotopes [8] down to the few percent level. For $^{105}_{46}\mathrm{Pd}_{59}$, these contributions should be of the order of 1%.

C. Seniority argument

As stated in the introductory remarks to this section, our argument is based on the concept that, for an odd nucleus, the wave function is dominated by seniority-1 components. This is not always the case; for example, in the $f_{7/2}$ shell, the spin-parity of ^{47}Ti is $\frac{5}{2}^-$ instead of $\frac{7}{2}^-$, and the $\frac{7}{2}^-$ ground state of ^{45}Ti is nearly degenerate with $\frac{5}{2}^-$ and $\frac{3}{2}^-$ states. Even in these cases, the validity of the seniority concept does not break down. In the MBZ wave function [16], the terms in the seniority expansion of the wave function drop off rapidly with increasing seniority. The concept of most nucleons being coupled in zero angular momentum pairs remains valid.

In Appendix A, we show that the analog matrix element for the one-body multipole operator Q_{IN} between seniority-1, $(2p+1)$-nucleon j-shell state vectors is closely related in magnitude to the corresponding one-nucleon matrix element. A seniority-1 state of $(2p+1)$ j-level nucleons has the same diagonal matrix element of a one-body operator of odd multipolarity I as the corresponding one-body amplitude [see the text following Eq. (A7) in Appendix A]. For all multipolarities ($I\neq0$), the result is

$$\langle(j)^{2p+1},v=1|\mathbf{Q}_{IN}|(j)^{2p+1},v=1\rangle=\langle(j)^1,v=1|\mathbf{Q}_{IN}|(j)^1,v=1\rangle\times\begin{cases}1 & \text{for odd } I\ ,\\ 1-2p/(\Omega-I) & \text{for even } 1\ ,\end{cases} \tag{16}$$

where $\Omega=(2j+1)/2$. The first factor on the right in Eq. (16) is just the one-particle matrix element. The numerical (second) factor varies between $+1$ for I odd, or $p=0$, and -1 for I even, $p=\Omega-1$. Similar results hold for transitions involving excitation from a seniority-1 state of one j to a seniority-1 state of another j.

What these results tell us is that, in contrast to $I=0$, there is no enhancement in the diagonal seniority-1 matrix element as a result of increasing particle number. The matrix element for many particles in the j level is equal to or less than that for one particle. Applied to Eq. (7), taking into account Eq. (16), this tells us that the effect of higher multipole operators on the cross section for analog transitions in odd-A nuclei is of the order of $(N-Z)^{-1}$, that is, of the order of $(N-Z)^{-2}$ relative to analog transitions.

D. Collective state admixtures

A possible breakdown of the seniority argument could come from consideration of collective admixtures. In odd nuclei, the zero-order ground state is the seniority-1 state consisting of one odd nucleon in some single-particle state and all other nucleons (the "core") coupled to angular-momentum-zero pairs. For a strong collective core in the presence of the extra particle, the physical ground state consists of a mixture of the seniority-1 state plus collective core states coupled with the single particle (in various j states) to the ground-state angular momentum. The strong admixtures are with one-phonon excitations, seniority-2 states of the core, which along with the odd particle give seniority-3 configurations of the nucleus. These are, however, special seniority-3 states, in

which two of the particles are in a constructively coherent mixture of seniority 2. Thus these components can have strong transitions which can overwhelm the single-particle contribution to $B(E\lambda)$. As an example, consider the simplest case of the nuclear ground state made up of a mixture of a seniority-1 state of angular momentum j and a collective quadrupole core coupled with various single-particle states j' to total angular momentum j. The state vector is of the form

$$\Psi=\sum_{nj'} C_{nj'}[\Phi_n(c)\psi_{j'}]_j \ , \tag{17}$$

where $\Phi_n(c)$ and $\psi_{j'}$ are the collective and particle parts of the wave function, respectively.

Using Eqs. (1), (2), (4), and (6), we can write the charge-exchange nuclear matrix element, including projectile isospin, as

$$\begin{aligned}\langle JMT,T-1,\tfrac{1}{2},\tfrac{1}{2}|V|JMTT,\tfrac{1}{2},-\tfrac{1}{2}\rangle \\ =\langle \tfrac{1}{2},\tfrac{1}{2}|\tau_+(0)|\tfrac{1}{2},-\tfrac{1}{2}\rangle (T)^{-1/2}\sum_{ISLN}(-1)^{N+1+I-S-L}\mathcal{Y}_{I(LS),-N}(\hat{r}_0) \\ \times\sum_i \langle JMTT|\mathcal{Y}_{I(\lambda S)N}(\hat{r}_i)F_{I(LS)\lambda 1}(r_0,r_i)\tau_0(i)|JMTT\rangle \ .\end{aligned} \tag{18}$$

The projectile isospin matrix element is 1.

We next estimate the collective contribution to analog charge exchange by first substituting Eq. (17) into Eq. (18), thus arguing that the cross terms involving a virtual collective transition between an unexcited core and a one-phonon core excitation are the dominant terms. In spite of the collectivity in the core states, the matrix elements are small because of the isovector nature of the operator acting between isoscalarlike collective excitations n in Eq. (17). Finally, we relate the cross section in the distorted-wave approximation (DWA) to the corresponding inelastic cross section for one-phonon excitation in the neighboring even "core" nucleus. The details of this procedure are carried out in Appendix C, with the final estimate

$$\frac{\sigma_{ce}}{\sigma_{in}}\le\frac{1}{T}\left[\frac{\beta_1 V_1}{\beta_0 V_0}\frac{N-Z}{A}\right]^2 , \tag{19}$$

where β_0 and β_1 are isoscalar and isovector deformation parameters, which may be defined as

$$\beta_0=\frac{N\beta_n+Z\beta_p}{N+Z}, \quad \beta_1=\frac{N\beta_n-Z\beta_p}{N-Z} \ . \tag{20}$$

We may write [19] the factor

$$\frac{\beta_1}{\beta_0}\frac{N-Z}{A}=\frac{N\beta_n-Z\beta_p}{N\beta_n+Z\beta_p}\frac{N+Z}{N-Z}\frac{N-Z}{A}=\frac{M_n-M_p}{M_n+M_p} \ , \tag{21}$$

where M_n and M_p are multipole matrix elements for neutrons and protons. A typical value of M_n/M_p is N/Z, and so

$$\frac{M_n-M_p}{M_n+M_p}\approx\frac{N-Z}{A} \ . \tag{22}$$

In the case of single-closed-shell nuclei, M_n/M_p can differ substantially from N/Z. In ^{48}Ca, for example, $M_n/M_p\approx 3$, and in ^{206}Pb it is about 2.5, which are quite extreme values. For the typical proton valence single-closed-shell nucleus ^{90}Zr, $M_n/M_p\approx 0.85$, and so the ratio $(M_n-M_p)/(M_n+M_p)\approx 0.2$. For our example of ^{105}Pd, it should be closer to $(N_c-Z_c)/A_c=\frac{12}{104}\approx 0.11$. The $\lambda=2$ contribution to charge exchange would then be for a typical ratio $V_1/V_0=\frac{1}{2}$ (see Ref. [20]) from Eq. (C11),

$$\sigma_{ce}(\lambda=2)\le\tfrac{2}{13}(\tfrac{1}{2}\times 0.11)^2\sigma_{\rm in} \ . \tag{23}$$

Using $\sigma_{\rm in}=30$ mb (see Ref. [21]) gives us $\sigma_{ce}(I=\lambda=2)=0.01$ mb, only about 0.003 times the experimental value of 3.75 mb (see Table II).

E. Multistep processes

It is well known [1] that transitions between ground states and their analogs in the low-energy (p,n) reaction are substantially reduced by destructive interference from three-step amplitudes involving two inelastic transitions and one charge exchange. Two-step processes are substantially smaller, as they involve an isovector inelastic transition, which we have seen in Sec. III D to be very weak. In addition, they are nearly incoherent with the one-step process, and so their contribution enters approximately as the square of the amplitude. Each three-step amplitude involves two strong isoscalar inelastic steps and one strong Fermi-like analog transition. The phases of the two intermediate Green's functions are each approximately $-i$, and so their product has phase -1 relative to the one-step process. This subtraction has a direct physical interpretation in terms of the loss of probability to the inelastic channels.

The question we address here is whether the spreading out of the intermediate collective states due to coupling to the intermediate particle can affect (reduce) the (negative) three-step contribution. A typical three-step route in the odd case is shown in Fig. 3, where the excited states J (and their analogs) are due to the mixing of a particle state with a strong collective inelastic state in the neighboring even nucleus.

The three-step processes, such as the one in Fig. 3, contribute an amplitude

$$A^{(3)}=\sum_{JJ'}\langle\Psi_A^0|\Delta V_C|\psi_A^{J'}\rangle\langle\psi_A^{J'}|\Delta V_{CE}|\psi^J\rangle\langle\psi^J|\Delta V_C|\Psi^0\rangle G_J G_{J'} , \tag{24}$$

where we have included only the collective part ΔV_C of the inelastic interaction. To a good approximation, the small differences in the energies of the inelastic states do not affect the intermediate projectile Green's function G_J, which may then be factored out of the JJ' sums. Using Eq. (17), we may write the inelastic sums as

$$\sum_J|\psi^J\rangle\langle\psi^J|=\sum_J\sum_{njn'j'}|n'j'\rangle\langle n'j'|J\rangle\langle J|nj\rangle\langle nj|=\sum_{nj}|nj\rangle\langle nj| , \tag{25}$$

where we have suppressed the projection quantum numbers. The sum over J and other quantum numbers gives $\delta_{nn'}\delta_{jj'}$, leaving

$$\sum_J|\psi^J\rangle\langle\psi^J|=\sum_{nj}|\Phi_{nJ_n}\psi_j\rangle\langle\Phi_{nJ_n}\psi_j| \tag{26}$$

and likewise the sum over J'. Thus the three-step amplitude can be written, using again Eq. (1) and writing out the coupled ground state,

$$A^{(3)}=(2T)^{-1/2}\sum_{njn'j'}\sum_{n_1j_1n_2j_2}C^0_{n_1j_1}C^{0*}_{n_2j_2}\langle\Phi_{n_2}\psi_{j_2}|\Delta V_C|\Phi_{n'}\psi_{j'}\rangle$$
$$\times\langle\Phi_{n'}\psi_{j'}|[T_+,\Delta V_{CE}]|\Phi_n\psi_j\rangle\langle\Phi_n\psi_j|\Delta V_C|\Phi_{n_1}\psi_{j_1}\rangle G(r,r')G(r',r'') . \tag{27}$$

Since we are including only the collective part of the inelastic interaction, ΔV_C, the j and j' are restricted to be equal to j_1 and j_2, respectively. Furthermore, as we showed in Sec. III D, an upper limit estimate of the $I=2$ contribution to the analog cross section is only about 0.3% of the $I=0$ contribution. Thus only the latter need be included for our estimate, which forces $n=n'$, $j=j'$. Also, because the $I=0$ (Fermi-like) charge-exchange matrix element is nearly model independent, we can equate the terms for various core excitations to that for unexcited core states, $n=n'=0$ and $j=J$, the angular momentum of the ground state. In addition, we now keep only the dominant zero- and one-quadrupole-phonon core excitations in the expansion. This leaves us with the two types of terms: those in which $n_1=n_2=0$ and $n=n'=1$ quadrupole phonon and those in which $n_1=n_2=1$ and $n=n'=0$ quadrupole phonon. These two types of collective inelastic matrix elements are equal within a phase, which cancels itself out between the two inelastic matrix element factors. All these approximations and manipulations leave us with the simple result

$$A^{(3)}=(2T)^{-1/2}\left[|C^0_{0j}|^2+\sum_{j'}|C^0_{2j'}|^2\right]$$
$$\times\langle\Phi_0|\Delta V_C|\Phi_{1,2}\rangle\langle\Phi_0\psi_j|[T_+,\Delta V_{CE}]|\Phi_0\psi_j\rangle$$
$$\times\langle\Phi_{1,2}|\Delta V_C|\Phi_0\rangle G(r,r')G(r',r'') , \tag{28}$$

where now j is taken to be the ground-state spin of the odd nucleus. The two terms in the bracket sum approximately to 1, as a result of the normalization of the ground-state wave function, leaving a result which is precisely that obtained for even nuclei. Thus, in these approximations, the three-step correction to analog transition strengths is expected to be the same as for even nuclei. It appears that there is no substantial reduction for odd nuclei in the three-step amplitudes which would be able to give rise to a large odd-even discrepancy in $\sigma/(N-Z)$.

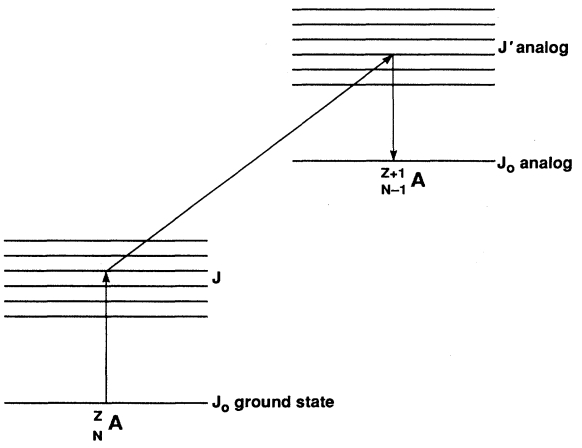

FIG. 3. Typical three-step route in an even-odd nucleus. The excited states J (and their analogs) are due to the mixing of a particle state with a strong collective inelastic state in the neighboring even-even nucleus. A, Z, and N are the mass number, proton number, and neutron number, respectively.

IV. DISCUSSION OF RESULTS

A. Ground-state analog transitions

In Fig. 2 the upper curve shows the differential cross section for the ^{105}Pd(p,n) reaction to the ground-state analog. The solid curves in Fig. 2 are not theoretical angular distributions; rather, they are Legendre fits to the angular distribution, used to determine total cross sections. In Fig. 4 the ratio $\sigma(p,n)$ for ^{105}Pd to the corresponding quantity of the two neighboring even isotopes has been plotted as a function of center-of-mass angle. (Note that the errors in Fig. 4 are smaller than those shown in Fig. 2, since some of the systematic errors cancel when taking the ratio of the cross sections.) The cross sections for the even isotopes have been compared to the

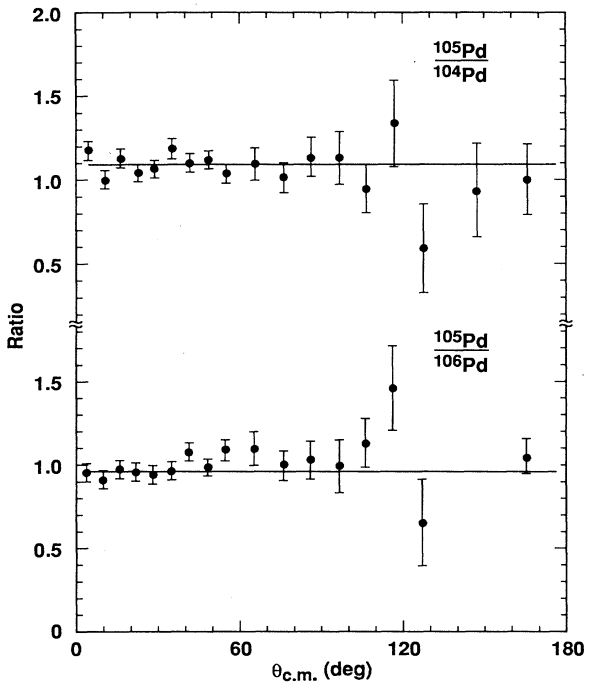

FIG. 4. Ratio of the ^{105}Pd$(p,n)^{105}$Ag ground-state analog cross section to the ^{104}Pd$(p,n)^{104}$Ag ground-state analog cross section (upper curve), and to the ^{106}Pd$(p,n)^{106}$Ag ground-state analog cross section (lower curve).

coupled-channels Lane model in Ref. [3]. It is clear that the angular distribution for the odd isotope is in good agreement with those of the even isotopes over nearly the whole angular range, failing only beyond 120°, where the analog differential cross section has already fallen by almost a factor of 100 from the value at 0°.

In the analysis of Sec. III, we have shown that, although higher multipole transitions ($I>0$) than the dominant Fermi-like ($I=0$) amplitude are possible for odd nuclei, there seems to be no direct mechanism for which these contributions are significant. This is in good agreement with our experimental results. Contributions from higher multipoles would not only increase the magnitude for odd nuclei compared to its even neighbors, but would also give different angular distributions, contrary to the plots shown in Fig. 4.

B. Excited analog transitions

The cross sections for the (p,n) excited analog states are also shown in Fig. 2. The nuclear structure in ^{105}Pd is somewhat complicated, following neither the vibrational nor rotational models. The even isotopes have a nearly perfect $0^+,2^+,4^+$ triplet above the first excited state, suggesting a harmonic vibration, but at an energy greater than double that of the first excited state, indicating a tendency toward rotational structure. Our attempts to reproduce this structure with an intermediate-coupling particle-core vibrational model have not been successful.

In even nuclei it has been well established [22,23] that at the projectile energies of our experiment, the 2^+ excited analog states are reached primarily by the two-step process involving (primarily) isoscalar collective inelastic excitation before or following a Fermi-like analog charge-exchange transition. The direct one-step excitation, being a collective matrix element of an isovector operator, is weak, as we have seen in Sec. III D, and typically negligible compared to the two-step process, in which both the charge-exchange and inelastic steps are strong. In medium and heavy nuclei, no analog states appear in the spectrum except those of collective states of the parent.

In this paper we content ourselves to make a comparison of the (p,n) cross section with the $B(E2)$ values for inelastic excitation of the parent states. Only the $\frac{7}{2}^+$ and $\frac{9}{2}^+$ states are clearly visible in the (p,n) spectrum of Fig. 1. For comparison, in Table I we display the $B(E2)$ values measured by Coulomb excitation [14,15]. The $\frac{7}{2}^+$ and $\frac{9}{2}^+$ states are by far the strongest electromagnetic transitions, and the $B(E2)$ values are approximately in the ratio 2 to 1, in good agreement with the ratio of our integrated cross sections given in Table II. The interpretation of the excited analog excitation as taking place through excitation of a collective inelastic state followed by a Fermi charge-exchange transition to its analog (or vice versa) appears to be well justified by our data.

V. SUMMARY AND CONCLUSION

We have measured the analog and excited analog ^{105}Pd(p,n) transitions at 26 MeV bombarding energy. Because the analog transition in odd nuclei can involve multipoles I of the interaction up to $2J$, where J is the angular momentum of the target ground state, we have made a detailed theoretical analysis of the transitions of higher multipolarity. We have shown that for a seniority-1 state of an odd nucleus, the analog matrix element falls off with increasing neutron excess as $1/(N-Z)^{1/2}$ compared to $(N-Z)^{1/2}$ for the $I=0$ amplitude. Since the cross section for different multipoles is approximately incoherent, the $I>0$ contributions to the cross section will be of the order of $1/(N-Z)^2$ relative to the $I=0$ contributions. We have also considered the effects of mixing of an extra-core particle with the collective excitations of the neighboring even nucleus. In shell-model terminology, these would be seniority-3 states with various particle-hole configurations constructively coherent for inelastic excitations. By writing the multipole of order I in terms of the collective amplitudes in the neighboring even nuclei and comparing those for charge exchange with those for inelastic scattering, we have made estimates that the collective effects are also negligible, primarily because the strong low-lying states are isoscalar, whereas the interaction is isovector. Effects of higher multipoles on the important three-step destructively coherent amplitudes were also studied; the result again was that higher multipoles of the interaction should not be significant. This theoretical conclusion is in good agreement with our experimental results, which show that not only the magnitude but also the differential cross section for analog transitions divided by the neutron excess agree in odd and even nuclei over the whole angular

range up to a center-of-mass angle of 120°, where the cross section has dropped off by two orders of magnitude from that at 0°.

The present study has examined the possibility that contributions from spin-flip, higher multipoles ($I>0$), collective admixtures, or multistep processes might enhance the analog cross sections for odd-A targets. Each of these contributions was found to be small enough that odd isotopes should follow the same systematics as a function of the deformation parameter and $(N-Z)$ as the even-A targets, although this may not be true for targets with $(N-Z)\leq 2$. This agrees with the present results for ^{105}Pd and previous results [5,6] for ^{97}Mo, but does not resolve the discrepancies found for ^{95}Mo, ^{47}Ti, and ^{49}Ti. In some of these cases (^{47}Ti and ^{95}Mo), an excited analog state was not resolved from the ground state, but this contribution was estimated to be small, based on the strength of the other excited analogs and on the consistency of the angular distribution with those of the even isotopes. Moreover, for ^{49}Ti all excited analogs are resolved from the ground state and the discrepancy still is observed.

Other interesting possibilities are the presence of nonanalog states very close to the analog in energy. Again, the absence of other strong nonanalog transitions in the vicinity of the analog argues against this explanation, but the proximity of nonanalog strength to the analog might vary somewhat irregularly with A, since the excitation energy of the analog in the residual nucleus varies considerably between neighboring isotopes in some situations.

Complicating the picture somewhat is the fact that of the even isotopes which have been studied at the most energies, those for titanium [8] and molybdenum [5,6] have shown energy dependences which are not completely understood. Thus the resolution of the anomalous cross sections for some odd-A isotopes could be associated with yet unexplained features of the energy dependence of the analog transition. It has been pointed out [8] that the energy dependence of the analog transition in this mass region is very sensitive to the diffuseness of the imaginary potential for nucleons in this energy range. This is presumably due to the substantial effect single-particle resonances can have on such transitions and the resultant dependence on the damping of these resonances. The effects of other giant resonances [5,6,8] in the compound system need to be investigated, as do the possible effects of the Fermi surface anomaly [24]. Finally, a more careful look at possible preequilibrium contributions [25] to the cross section should be taken, although these would likely not have the resonancelike feature observed in some of the cross sections.

Some details of the behavior of the (p,n) cross section to analog states remain unclear. Additional theoretical work on the topics previously listed would be useful, as would more detailed experimental studies of the energy dependence and possible even-A, odd-A differences in the 30–60 MeV bombarding energy range.

ACKNOWLEDGMENTS

This work was performed under the auspices of the U.S. Department of Energy by the Lawrence Livermore National Laboratory under Contract No. W-7405-ENG-48. It was also supported at the University of Hamburg by the German Federal Ministry of Research and Technology (BMFT) under Contract No. 06-HH-142.

APPENDIX A: TRANSITION STRENGTHS WITH SENIORITY WAVE FUNCTIONS

Our object is to try to calculate a transition amplitude for a partially filled shell. Define the coupled two-particle creation operator

$$A^{\dagger}_{\mathrm{IN}}(j_1,j_2)=\sum_{m_1m_2}\langle j_1j_2m_1m_2|IN\rangle a^{\dagger}_{j_2m_2}a^{\dagger}_{j_1m_1} \tag{A1}$$

and the transition operator for angular momentum transfer I,

$$A^{0}_{IN}(j_1,j_2)=\sum_{m_1m_2}\langle jjm_1-m_2|I-N\rangle(-1)^{j-m_1}a^{\dagger}_{j_2m_2}a_{j_1m_1}\ , \tag{A2}$$

and let $A^{\dagger}=A^{\dagger}_{00}(jj)$, where j is some principal filling level. We will consider a partially filled shell of seniority 1:

$$\Psi=\mathbb{N}A^{\dagger p}a^{\dagger}_{j_1m_1}|0\rangle\ , \tag{A3}$$

where $|0\rangle$ is a state of lower filled shells, the operator $A^{\dagger p}$ creates an additional $2p$ particles coupled to p angular-momentum-zero pairs, and N normalizes Eq. (A3). First, consider the simpler case in which $j_1\neq j$ and $j_2\neq j$. The transition matrix element is

$$\begin{aligned}\mathbb{N}^2\langle 0|a_{j_2m_2}A^{p}A^{0}_{\lambda\mu}(j_1,j_2)A^{\dagger p}a^{\dagger}_{j_1m_1}|0\rangle&\\ =\mathbb{N}^2\langle 0|a_{j_2m_2}A^{0}_{\lambda\mu}(j_1j_2)a^{\dagger}_{j_1m_1}|0\rangle\langle 0|A^{p}A^{\dagger p}|0\rangle&\\ =\langle 0|a_{j_2m_2}A^{0}_{\lambda\mu}(j_1j_2)a^{\dagger}_{j_1m_1}|0\rangle\ .&\end{aligned} \tag{A4}$$

Equation (A3) tells us that the transition matrix element for $2p+1$ particles is precisely the same as for 1 particle.

Next, consider transition matrix elements of the nontrivial type involving the operator $A^{0}_{\lambda\mu}\equiv A^{0}_{\lambda\mu}(j,j)$ between states of $2p+1$ particles in a single shell,

$$\mathbb{N}^2\langle 0|a_{jm'}A^{p}A^{0}_{\lambda\mu}A^{\dagger p}a^{\dagger}_{jm}|0\rangle\ . \tag{A5}$$

We may develop the operator product

$$\begin{aligned}A^{p}A^{0}_{\lambda\mu}A^{\dagger p}&=A^{p-1}\{[A,A^{0}_{\lambda\mu}]+A^{0}_{\lambda\mu}A\}A^{\dagger p}\\ &=A^{p-2}\{[A,[A,A^{0}_{\lambda\mu}]]+[A,A^{0}_{\lambda\mu}]A\\ &\quad+[A,A^{0}_{\lambda\mu}]A+A^{0}_{\lambda\mu}A^{2}\}A^{\dagger p}\ .\end{aligned} \tag{A6}$$

The double commutator is zero, as both A and $[A,A^{0}_{\lambda\mu}]$ contain only destruction operators [see Eq. (B7)]. Thus Eq. (A6) becomes

$$A^p A^0_{\lambda\mu} A^{\dagger p} = A^{p-2}\{2[A, A^0_{\lambda\mu}]A + A^0_{\lambda\mu}A^2\}A^{\dagger p}$$
$$= A^{p-3}\{2[A, A^0_{\lambda\mu}]A^2 + [A, A^0_{\lambda\mu}]A^2 + A^0_{\lambda\mu}A^3\}A^{\dagger p}$$
$$= p\frac{2(-1)^\mu}{\hat{j}} A_{\lambda-\mu} A^{p-1} A^{\dagger p} + A^0_{\lambda\mu} A^p A^{\dagger p} . \tag{A7}$$

For λ odd, the operator $A_{\lambda\mu}$ in the first term is identically zero [see Eq. (A1)], leaving us with the simple result

$$\mathbb{N}^2\langle 0|a_{jm'} A^p A^0_{\lambda\mu} A^{\dagger p} a^\dagger_{jm}|0\rangle = \mathbb{N}^2\langle 0|a_{jm'} A^0_{\lambda\mu} A^p A^{\dagger p} a^\dagger_{jm}|0\rangle . \tag{A8}$$

This matrix element may be reduced by commuting A past $A^{\dagger p}$ exactly as was done for the calculation of the normalization coefficient $\mathbb{N}$ in Eq. (B12). The numerical factors which come from such a procedure then exactly cancel the $\mathbb{N}^2$, giving us

$$\mathbb{N}^2\langle 0|a_{jm'} A^p A^0_{\lambda\mu} A^{\dagger p} a^\dagger_{jm}|0\rangle = \langle 0|a_{jm'} A^0_{\lambda\mu} a^\dagger_{jm}|0\rangle . \tag{A9}$$

In other words, the transition matrix element for λ odd for the $2p+1$ particle seniority-1 state is exactly equal to that for the corresponding one-particle (necessarily seniority-1) state.

For even values of λ, the second term of Eq. (A7) may now be treated exactly as the normalization matrix element Eqs. (B9)–(B13), eventually giving back just the matrix element for a single particle in the j level. The first term of Eq. (A7), which we now concentrate on, is the correction due to the additional p pairs in the nucleus. It is a large correction for nearly filled levels.

Our next task is to move one $A^\dagger$ past A^{p-1}, eventually commuting it past the $A_{\lambda-\mu}$ in the matrix element of the first term of Eq. (A7),

$$\langle 0|a_{jm'} A_{\lambda-\mu} A^{p-1} A^\dagger A^{\dagger p-1} a^\dagger_{jm}|0\rangle . \tag{A10}$$

We may write

$$A^{p-1}A^\dagger = A^{p-2}[A, A^\dagger] + A^{p-2}A^\dagger A$$
$$= A^{p-2}[A, A^\dagger] + A^{p-3}[A, A^\dagger]A + A^{p-4}[A, A^\dagger]A^2 + \cdots + [A, A^\dagger]A^{p-2} + A^\dagger A^{p-1}$$
$$= \frac{2}{\Omega}\{A^{p-2}(\Omega - N) + A^{p-3}(\Omega - N)A + \cdots + (\Omega - N)A^{p-2}\} + A^\dagger A^{p-1} , \tag{A11}$$

where N is the number operator for j-level nucleons. Inserted into Eq. (A10), this series (in curly brackets) will give

$$\frac{2}{\Omega} A^{p-2}\{(\Omega - 2p + 2 - 1) + (\Omega - 2p + 4 - 1) + \cdots + [\Omega - 2p + 2(p-1) - 1]\}$$
$$= \frac{2}{\Omega} A^{p-2}\{(p-1)(\Omega - 2p - 1) + (p-1)p\} = \frac{2}{\Omega}(p-1)(\Omega - p - 1)A^{p-2} . \tag{A12}$$

Thus Eq. (A10) is

$$\langle 0|a_{jm'} A_{\lambda-\mu}\left\{\frac{2}{\Omega}(p-1)(\Omega - p - 1)A^{p-2} + A^\dagger A^{p-1}\right\} + A^{\dagger p-1} a^\dagger_{jm}|0\rangle . \tag{A13}$$

The second term is the type we want; the first is just like Eq. (A10) with p replaced by $(p-1)$. We may then continue the process with the *first term* of Eq. (A13) to get

$$\langle 0|a_{jm'} A_{\lambda-\mu} A^\dagger \left\{A^{p-1}A^{\dagger p-1} + \frac{2}{\Omega}(p-1)(\Omega - p - 1)A^{p-2}A^{\dagger p-2}\right.$$
$$+ \frac{2}{\Omega}(p-1)(\Omega - p - 1)\frac{2}{\Omega}(p-2)(\Omega - p)A^{p-3}A^{\dagger p-3} + \cdots$$
$$\left. + \frac{2}{\Omega}(p-1)(\Omega - p - 1)\frac{2}{\Omega}(p-2)(\Omega - p)\cdots\frac{2}{\Omega}(1)(\Omega - 3)\right\} a^\dagger_{jm}|0\rangle . \tag{A14}$$

The general term in the curly brackets of Eq. (A14) is then

$$A^{p-m}A^{\dagger p-m}\left[\frac{2}{\Omega}\right]^{m-1}(p-1)(p-2)\cdots(p-m+1)(\Omega - p - 1)(\Omega - p)\cdots(\Omega - p + m - 3)$$
$$= A^{p-m}A^{\dagger p-m}\left[\frac{2}{\Omega}\right]^{m-1}\frac{(p-1)!}{(p-m)!}\frac{(\Omega - p + m - 3)!}{(\Omega - p - 2)!} . \tag{A15}$$

The evaluation for the operators $A^{p-m}A^{\dagger p-m}$ is carried out in the same way as in the normalization constant (B12): The general term is

$$\langle 0|a_{jm'}A_{\lambda-\mu}A^{\dagger}A^{p-m}A^{\dagger p-m}a^{\dagger}_{jm}|0\rangle=\left[\frac{2}{\Omega}\right]^{p-m}\frac{(p-m)!(\Omega-1)!}{(\Omega-1-p+m)!}\langle 0|a_{jm'}A_{\lambda-\mu}A^{\dagger}a^{\dagger}_{jm}|0\rangle\ . \tag{16}$$

Combining Eq. (A15) with Eq. (A16), we get, for the general term of Eq. (A14),

$$\langle 0|a_{jm'}A_{\lambda-\mu}A^{\dagger}A^{p-m}A^{\dagger p-m}|0\rangle=\left[\frac{2}{\Omega}\right]^{p-1}\frac{(\Omega-1)!(p-1)!\langle 0|a_{jm'}A_{\lambda-\mu}A^{\dagger}a^{\dagger}_{jm}|0\rangle}{(\Omega-p+m-1)(\Omega-p+m-2)(\Omega-p-2)!}\ . \tag{A17}$$

As all terms of Eq. (A17) multiply a common matrix element, we sum the terms $m=1$ to $m=p$ to give an overall coefficient for Eq. (A10),

$$\left[\frac{2}{\Omega}\right]^{p-1}\frac{(\Omega-1)!(p-1)!}{(\Omega-p)!}\times\sum_{m=1}^{p}\frac{(\Omega-p)(\Omega-p-1)}{(\Omega-p+m-1)(\Omega-p+m-2)}=\left[\frac{2}{\Omega}\right]^{p-1}\frac{(\Omega-2)!p!}{\Omega-1}\ . \tag{A18}$$

Now that we have a pair creation operator next to $A_{\lambda-\mu}$ in Eq. (A17), we anticommmute it,

$$A_{\lambda-\mu}A^{\dagger}=[A_{\lambda-\mu},A^{\dagger}]+A^{\dagger}A_{\lambda\mu}=-\frac{4}{\hat{j}}(-1)^{\mu}A^{0}_{\lambda\mu}+A^{\dagger}A_{\lambda\mu}\ . \tag{A19}$$

Note that it is the vanishing of the first term of Eq. (B3) in the commutator of Eq. (A19) that distinguishes all the higher multipoles from $\lambda=0$. The second term gives zero in the matrix element, and the first gives us our original transition operator just to the right of the single-particle destruction operator, multiplied by a sum of terms with pair products.

All these results, Eqs. (A5), (A7), (A10), (A14), (A15), (A18), (A19), and (B12), together give

$$\langle\Psi'_{v=1}|A^{0}_{\lambda\mu}|\Psi_{v=1}\rangle=\left[\frac{\Omega}{2}\right]^{p}\frac{1}{p!}\frac{(\Omega-1-p)!}{(\Omega-1)!}\times\langle 0|a_{jm'}A^{p}A^{0}_{\lambda\mu}A^{\dagger p}a^{\dagger}_{jm}|0\rangle=\left[1-\frac{2p}{\Omega-1}\right]\langle 0|a_{jm'}A^{0}_{IN}a^{\dagger}_{jm}|0\rangle\ . \tag{A20}$$

In other words, the seniority 1 $(2p+1)$ j-shell nucleon diagonal matrix element for the even $I\neq 0$ multipole transition operators is the numerical factor $[1-2p/(\Omega-1)]$ times the corresponding one-particle matrix element. The spectroscopic amplitude [26], defined generally as

$$S(J_iJ_fI;j_1j_2\alpha_1\alpha_2)=\frac{\langle J_f\|A^{0}_{I}(j_1j_2\alpha_1\alpha_2)\|J_i\rangle}{\hat{I}}\ , \tag{A21}$$

for Eq. (A20) is therefore

$$S(jjI;jj\alpha\alpha)=1-\frac{2p}{\Omega-1}\ , \tag{A22}$$

since, by definition, the spectroscopic amplitude for a single-particle transition is 1. In Eqs. (A21) and (A22), α is the single-particle isospin index.

For odd λ there are no correction terms, and so the net numerical factor is trivially $+1$, correct result for a one-hole state. The spectroscopic amplitude for even λ can be written

$$1-\frac{2p}{\Omega-1}=\frac{p_m-2p}{p_m}\ , \tag{A23}$$

where $p_m=\Omega-1$ is the maximum number of pairs possible for a seniority-1 state. This factor varies between $+1$ for $p=0$ to -1 for $p=p_m$, vanishing for $p=\frac{1}{2}p_m=\frac{1}{2}(j-\frac{1}{2})$ (which can occur for $j=2n+\frac{1}{2}$, where n is an integer). As a check, the value -1 for $p=p_m$ is the correct result for a one-hole state.

Two other useful results can be obtained for transitions from a seniority-1 state of one single particle to a seniority-1 state of another. The first involves the transfer of an odd particle to another j value,

$$M_{fi}=\langle 0|a_{j'm'}A^{p'}(j')A^{p}(j)A^{0}_{\lambda\mu}(jj')A^{\dagger p'}(j')A^{\dagger p}(j)a^{\dagger}_{jm}|0\rangle\mathbb{N}_j(1,2p+1)\mathbb{N}_j(0,2p)\mathbb{N}_{j'}(0,2p')\mathbb{N}'_j(1,2p'+1)\ , \tag{A24}$$

where $\mathbb{N}(v,2p+1)$ is the normalization factor for a state of seniority v of $2p+v$ particles.

The matrix element in Eq. (A24) may be written

$$\sum_{m_1m_2}\langle jj'm_1-m_2|\lambda-\mu\rangle(-1)^{j-m_1}\langle 0|a_{j'm'}A^{p'}(j')A^{p}(j)a^{\dagger}_{j'm_2}a_{jm_1}A^{\dagger}(j)^{p'}A^{\dagger}(j)^{p}a^{\dagger}_{jm}|0\rangle\ . \tag{A25}$$

Factoring the matrix element and commuting with A, we may write Eq. (A25) as

$$M_{fi}=\sum_{m_1m_2}\langle jj'm_1-m_2|\lambda-\mu\rangle(-1)^{j-m_1}\langle 0|a_{j'm'}A(j')^{p'}A^{\dagger}(j')^{p}a_{j'm_2}|0\rangle\langle 0|a_{jm_1}A(j)^{p}A^{\dagger}(j)^{p}a_{jm}|0\rangle$$

$$=\langle jj'm-m'|\lambda-\mu\rangle(-1)^{j-m_1}O_j(1,2p+1)O_{j'}(1,2p'+1)\ , \tag{A26}$$

where

$$O_j(v,2p+v)=\left[\frac{2}{\Omega}\right]^p p!\frac{(\Omega-v)!}{(\Omega-v-p)!} \tag{A27}$$

is derived in Appendix B, Eq. (B12).

The spectroscopic amplitude is then

$$S(jj'\lambda;jj'\alpha\alpha)=\left[\frac{2}{\Omega_j}\right]^p\left[\frac{2}{\Omega_j'}\right]^{p'}p!p'!\frac{(\Omega-1)!}{(\Omega-1-p)!}\frac{(\Omega'-1)!}{(\Omega-1-p')!}\mathbb{N}_j(0,2p)\mathbb{N}_j(1,2p+1)\mathbb{N}_j(0,2p')\mathbb{N}_{j'}(1,2p'+1)$$

$$=\left[\frac{(\Omega-p)(\Omega'-p')}{\Omega\Omega'}\right]^{1/2}. \tag{A28}$$

As $p<\Omega$, this spectroscopic factor is always less than 1.

The other matrix element of interest uses the same initial state as Eq. (A24), but increases the number of j particles,

$$M_{fi}=\langle 0|A^{p-1}(j)a_{j'm'}A^{p'-1}(j')A^{0}_{\lambda\mu}(j_1'j_2')A^{\dagger p'}(j')A^{\dagger p}a^{\dagger}_{jm}|0\rangle$$

$$\times\mathbb{N}(0,2p+2)\mathbb{N}(1,2p'-1)\mathbb{N}(0,2p')\mathbb{N}(1,2p+1)\ . \tag{A29}$$

The matrix element in Eq. (A29) is

$$\sum_{m_1m_2}\langle j_1j_2m_1-m_2|\lambda-\mu\rangle(-1)^{j-m_1}\langle 0|A^{p+1}(j)a_{j'm'}A^{p-1}(j')a^{\dagger}_{j_2m_2}a_{j_1m_1}A^{\dagger p'}(j')A^{\dagger p}(j)a^{\dagger}_{jm}|0\rangle$$

$$=\sum_{m_1m_2}-\langle j_1j_2m_1-m_2|\lambda-\mu\rangle(-1)^{j-m_1}\langle 0|A^{p+1}(j)a^{\dagger}_{j_2m_2}A^{\dagger p}(j)a^{\dagger}_{jm}|0\rangle\langle 0|a_{jm'}A^{p'-1}(j')a_{j_1m_1}A^{\dagger}(j')^{p'}|0\rangle\ . \tag{A30}$$

Putting in the normalization factors from Eq. (A29) gives

$$S(jj'\lambda;jj'\alpha\alpha)=(-1)^{-j'-j+\lambda}\frac{1}{\hat{j}\hat{j}'}\mathbb{N}(0,2p')\mathbb{N}(1,2p+1)\mathbb{N}(0,2p+2)\mathbb{N}(1,2p'-1)O(0,2p+2)O(0,2p')$$

$$=(-1)^{-j'-j+\lambda}\left[\frac{p'(p+1)}{\Omega'\Omega}\right]^{1/2}. \tag{A31}$$

Since the number of pairs ($p+1$ in the final state) is less than or equal to Ω, this matrix element is also always less than one in magnitude.

All these results, Eqs. (A4), (A22), (A28), and (A31), show that for seniority-1 state vectors there is no enhancement due to numbers of particles for any multiparity transition greater than 0. The only departure from the single-particle result of spectroscopic amplitude 1 is a reduction.

APPENDIX B: COMMUTATORS AND NORMALIZATION

The most often used commutator of the operators defined in Eqs. (A1) and (A2) is $[A,A^{\dagger}]$. As we will also need $[A_{\lambda\mu},A^{\dagger}]$, we may calculate the latter first and then specialize to $\lambda=\mu=0$. First note that $A_{\lambda\mu}\equiv 0$ for odd λ because of the fermion commutation relations. Thus the odd-λ case of the commutator is trivial, and we need consider only even values of λ in deriving the commutator. Thus we have

$$[A_{\lambda\mu}, A^\dagger] = \sum_{m_1 m_2 m_1' m_2'} \langle jjm_1' m_2' | \lambda\mu \rangle \langle jjm_1 m_2 | 00 \rangle [a_{jm_1} a_{jm_2}, a^\dagger_{jm_2'} a^\dagger_{jm_1'}]$$

$$= \sum_{m_1 m_2 m_1' m_2'} \langle jjm_1' m_2' | \lambda\mu \rangle \langle jjm_1 m_2 | 00 \rangle [\delta_{m_1 m_1'} \delta_{m_2 m_2'} - \delta_{m_1 m_2'} \delta_{m_2 m_1'} - \delta_{m_2 m_2'} a^\dagger_{jm_1'} a_{jm_1}$$

$$- \delta_{m_1 m_1'} a^\dagger_{jm_2'} a_{jm_2} + \delta_{m_2 m_1'} a^\dagger_{jm_2'} a_{jm_1} + \delta_{m_1 m_2'} a^\dagger_{jm_1'} a_{jm_2}] \ . \tag{B1}$$

Gathering like terms, using Eq. (A2), the orthogonality of the Clebsch-Gordan coefficients, and the value of the coefficient,

$$\langle jjm_1 m_2 | 00 \rangle = \frac{(-1)^{j-m_1}}{\hat{j}} \delta_{m_1, -m_2} \ , \tag{B2}$$

give finally the result

$$[A_{\lambda\mu}, A^\dagger] = 2 \left\{ \delta_{\lambda 0} - \frac{2(-1)^\mu}{\hat{j}} A^0_{\lambda-\mu} \right\} . \tag{B3}$$

For $\lambda = 0$, this is

$$[A, A^\dagger] = 2 \left\{ 1 - \frac{2(-1)^\mu}{\hat{j}} A^0 \right\} = 2 \left\{ 1 - \frac{2}{\hat{j}^2} N_j \right\} = 2 \left\{ 1 - \frac{N_j}{\Omega} \right\} , \tag{B4}$$

where $\Omega = (2j+1)/2$ and N is the j-level number operator, since

$$A^0 \equiv A^0_{00} = \sum_{m_1 m_2} \langle jjm_1 - m_2 | 00 \rangle (-1)^{j-m_1} a^\dagger_{jm_2} a_{jm_1} = \sum_{m_1 m_2} \frac{1}{\hat{j}} \delta_{m_1 m_2} a^\dagger_{jm_2} a_{jm_1} = \frac{1}{\hat{j}} N \ . \tag{B5}$$

The other important commutation relation is

$$[A, A^0_{\lambda\mu}] = \sum_{m_1 m_2 m_1' m_2'} \langle jjm_1 m_2 | 00 \rangle \langle jjm_1' - m_2' | \lambda - \mu \rangle (-1)^{j-m_1'} [a_{jm_1} a_{jm_2}, a^\dagger_{jm_2'} a_{jm_1'}]$$

$$= \sum_{m_1 m_2 m_1' m_2'} \frac{(-1)^{j-m_1}}{\hat{j}} \delta_{m_1, -m_2} \langle jjm_1' - m_2' | \lambda - \mu \rangle (-1)^{j-m_1'} [\delta_{m_2 m_2'} a_{jm_1} a_{jm_1'} - \delta_{m_1 m_2'} a_{jm_2} a_{jm_1'}] \ . \tag{B6}$$

Gathering like terms together gives finally the desired commutator

$$[A, A^0_{\lambda\mu}] = \begin{cases} \dfrac{2(-1)^\mu}{\hat{j}} A_{\lambda-\mu}, & \lambda \text{ even} \\ 0, & \lambda \text{ odd} \ . \end{cases} \tag{B7}$$

Normalization of a seniority wave function

$$\Psi = \mathbb{N} A^{\dagger p} \Psi_v \tag{B8}$$

requires that

$$N^2 \langle \Psi_v | A^p A^{\dagger p} | \Psi_v \rangle = 1 \ , \tag{B9}$$

where p is the number of pairs of nucleons coupled to zero added to a maximum seniority state of v particles. Using Eq. (B4), we may write

$$\langle \Psi_v | A^p A^{\dagger p} | \Psi_v \rangle = \langle \Psi_v | A^{p-1} \{ [A, A^\dagger] + A^\dagger A \} A^{\dagger p-1} | \Psi_v \rangle$$

$$= \langle \Psi_v | A^{p-1} \{ [A, A^\dagger] A^{\dagger p-1} + A^\dagger [A, A^\dagger] A^{\dagger p-2} + A^{\dagger 2} [A, A^\dagger] A^{\dagger p-3}$$

$$+ \cdots + A^{\dagger p-1} [A, A^\dagger] \} | \Psi_v \rangle$$

$$= \frac{2}{\Omega} \langle \Psi_v | A^{p-1} (\Omega - N) A^{\dagger p-1} + A^{p-1} A^\dagger (\Omega - N) A^{\dagger p-2} + \cdots + A^{p-1} A^{\dagger p-1} (\Omega - N) | \Psi_v \rangle \ . \tag{B10}$$

The state vectors $A^{\dagger p-n} \Psi_v$ are all eigenstates of the number operator, giving, for Eq. (B10),

$$\langle\Psi_v|A^pA^{\dagger p}|\Psi_v\rangle=\frac{2}{\Omega}\{(\Omega-v-2p+2)+(\Omega_j-v-2p+4)+\cdots+(\Omega-v)\}\langle\Psi_v|A^{p-1}A^{\dagger p-1}|\Psi_v\rangle$$
$$=\frac{2}{\Omega}(\Omega-v-p+1)p\langle\Psi_v|A^{p-1}A^{\dagger p-1}|\Psi_v\rangle\ . \tag{B11}$$

Repeating the procedure with $p\rightarrow p-1,\ldots,$ gives

$$\langle\Psi_v|A^pA^{\dagger p}|\Psi_v\rangle=\left[\frac{2}{\Omega}\right]^p p!\frac{(\Omega-v)!}{(\Omega-v-p)!}=O(v,2p+v)\ , \tag{B12}$$

assuming that Ψ_v is itself normalized. We therefore have

$$\Psi=\left[\left[\frac{\Omega}{2}\right]^p\frac{(\Omega-v-p)!}{(\Omega-v)!p!}\right]^{1/2}A^{\dagger p}\Psi_v\ . \tag{B13}$$

APPENDIX C: VIRTUAL EXCITATIONS OF COLLECTIVE STATES

In this appendix we use a collective model to estimate the effects of virtual excitations of collective states of the neighboring even-core nucleus by interaction with the odd nucleon. The development starts with the substitution of the coupled nuclear wave function into the charge-exchange matrix element, Eq. (18), giving

$$\langle JMT,T-1,\tfrac{1}{2},\tfrac{1}{2}|V|JMTT,\tfrac{1}{2},-\tfrac{1}{2}\rangle$$
$$=(T^{-1/2})\sum_{njn'j'}C_{nj}C^*_{n'j'}\sum_{ISLN}(-1)^{N+1+I-S-L}\mathcal{Y}_{I(LS),-N}(\hat{r}_0)\langle JJM,-M|I-N\rangle$$
$$\times(-1)^{I-N}\frac{1}{\hat{J}}\left\langle J(n'j')TT\left|\left|\sum_i\mathcal{Y}_{I(\lambda S)N}(\hat{r}_i)F_{I(\lambda S)1}(r_0,r_i)\tau_0\right|\right|J(nj)TT\right\rangle\ . \tag{C1}$$

As we are interested in collective contributions, we neglect the single-particle part of the operator in the nuclear matrix element. To this approximation we have

$$\left\langle J(n'j')TT\left|\left|\sum_i\mathcal{Y}_{I(\lambda S)N}(\hat{r}_i)F_{I(\lambda S)1}(r_0,r_i)\tau_0\right|\right|J(nj)TT\right\rangle$$
$$\approx\langle J(n'j')TT|Q_{I(\lambda S)N,10}(c)|J(nj)TT\rangle$$
$$=\delta_{jj'}(-1)^{j+I-J_c-J}(2J+1)W(J_cJJ_cJ;jI)\langle n_c'J_c'T_c\|Q_{I(\lambda S),1}(c)\|n_cJ_cT_c\rangle\ , \tag{C2}$$

where $Q_{I(\lambda S)N,10}(c)$ is the collective part of the isovector operator in the matrix element of Eq. (C1). Equation (C2) applies in cases where the extra-core particle is a neutron. If it is a proton, there is an additional isospin Clebsch-Gordan factor approximately equal to 1, which makes no difference for our purposes.

In Eq. (C2) there are two types of terms which we must consider: those with $n_c'=n_c$ and those with $n_c'\neq n_c$. Of the latter the dominant terms are those with the phonon number changing by one unit. For the low-lying states in odd nuclei, because of the mixing coefficients C_{nj}, the largest terms will be those involving one phonon of multipolarity I. The strongest collective excitations are those of the electric type, particulary $\lambda^\pi=2^+,3^-$, and so $I(\lambda S)=I(\lambda 0)=\lambda(\lambda 0)$ for a state $J(j\lambda)=j(j\lambda)$, giving, for Eq. (C1),

$$\langle jmT,T-1,\tfrac{1}{2},\tfrac{1}{2}|V|jmTT,\tfrac{1}{2},-\tfrac{1}{2}\rangle$$
$$=(T^{-1/2})\sum_N\mathcal{Y}_{\lambda,-N}(\hat{r}_0)\langle jjm,-m|\lambda-N\rangle(-1)^{j-m}$$
$$\times[C^2_{\lambda j}\langle j(j\lambda)TT\|Q_{\lambda,10}(c)\|j(j\lambda)TT\rangle+2C_{0j}C_{\lambda j}\langle j(j\lambda)T_cT_c\|Q_{\lambda,10}(c)\|j(j0)TT\rangle]$$
$$=(2j+1)(T^{-1/2})\sum_N\mathcal{Y}_{\lambda,-N}(\hat{r}_0)\langle jjm,m'|\lambda-N\rangle(-1)^{j-m}$$
$$\times[C^2_{\lambda j}W(\lambda j\lambda j;j\lambda)\langle\lambda T_cT_c\|Q_{\lambda,10}(c)\|\lambda T_cT_c\rangle$$
$$+2C_{0j}C_{\lambda j}(-1)^\lambda W(0j\lambda j;j\lambda)\langle\lambda T_cT_c\|Q_{\lambda,10}(c)\|0T_cT_c\rangle]\ . \tag{C3}$$

In the collective model, neglecting the difference between the isoscalar deformation parameter β_0 and the mass deformation parameter, we may write the isovector operator as [27,28]

$$Q_{\lambda N,10}(c)=-\frac{\beta_1}{\beta_0}R\frac{N-Z}{A}\frac{dV_1}{dr}\alpha_{\lambda N}\ , \tag{C4}$$

where $\alpha_{\lambda N}$ is the expansion parameter of the radius

$$R = R_0 \left[1 + \sum_{\lambda\nu} \alpha_{\lambda\nu} Y_{\lambda\nu}(\theta,\phi) \right] \tag{C5}$$

and V_1 is the isovector projectile-target interaction. Both R and $\alpha_{\lambda N}$ become dynamical operators when the surface is quantized. The isovector deformation parameter β_1 is allowed to be different from β_0 or, equivalently, $\beta_n \neq \beta_p$, to take into account shell effects on the isospin structure of the excitation.

Within the collective model, we may relate the isoscalar and isovector operators approximately by the relation

$$Q_{\lambda N,10} = -\frac{\beta_1 V_1}{\beta_0 V_0} \frac{N-Z}{A} Q_{\lambda N,00} \ . \tag{C6}$$

For a harmonic vibrator, the first term of Eq. (C3) is zero. We can get an order of magnitude upper limit on its contribution by taking the nonzero value of the first term in the rotational model for which

$$\frac{\langle \lambda \| \alpha_\lambda \| \lambda \rangle}{\langle \lambda \| \alpha_\lambda \| 0 \rangle} = (-1)^\lambda (\hat{\lambda}) \langle \lambda\lambda 00 | \lambda 0 \rangle \ , \tag{C7}$$

which is equal to -0.535 for $\lambda=2$, and 0 for $\lambda=3$. In addition, the Racah coefficient and the coupling coefficient for the first term of Eq. (C3) are typically smaller than the second term. For an estimate of the magnitude of the collective isovector contribution to analog transitions, we may therefore confidently neglect the diagonal (first) term of Eq. (C3) and consider only the second term, whose nuclear matrix element involves the transition from an unexcited core state to the one-photon state of multipolarity λ. This observation allows us to relate the collective contribution in charge exchange for an odd nucleus to inelastic excitation of the same core state in the neighboring even-core nucleus. The fact that different total angular momentum transfers allowed in the $j \to j$ ground-state transition are incoherent in the total cross section allows us to make the comparison of the partial cross section to the cross section for excitation of the λ-pole inelastic cross section in the neighboring core nucleus.

The inelastic scattering matrix element for the neighboring core nucleus for excitation of the one-photon state of multipolarity λ is

$$\begin{aligned} \langle \lambda M T_c T_c | V | 00 T_c T_c \rangle &= \sum_N (-1)^N \mathcal{Y}_{\lambda,-N}(\hat{r}_0) \left\langle \lambda M T_c T_c \left| \sum_i \mathcal{Y}_{\lambda N}(\hat{r}_i) F_\lambda(r_0, r_i) \right| 00 T_c T_c \right\rangle \\ &= (-1)^M \mathcal{Y}_{\lambda,M}(\hat{r}_0)(\hat{\lambda})^{-1} \langle \lambda T_c T_c \| Q_{\lambda,0}(c) \| 0 T_c T_c \rangle \ . \end{aligned} \tag{C8}$$

In Eq. (C8) we have included only the dominant isoscalar part of the nuclear operator, thus neglecting terms of order $(N-Z)/A$.

The cross section is obtained by taking the distorted wave (DW) matrix element of the nuclear matrix element Eq. (C8) multiplying by $(-2m/4\pi\hbar^2)$, squaring, and multiplying by k'/k, the ratio of the final to initial wave numbers and summing over final ones. The inelastic integrated cross section, neglecting spin-orbit effects, is therefore

$$\begin{aligned} \sigma_{in} = \int d\Omega' (2m/4\pi\hbar^2)^2 (k'/k)(\hat{\lambda})^{-2} \\ \times \sum_M | \langle \chi_f(\hat{r}_0) | (-1)^M \mathcal{Y}_{\lambda M}(r_0) \langle \lambda T_c T_c \| Q_{\lambda,00}(c) \| 0 T_c T_c \rangle | \chi_i(\hat{r}_0) \rangle |^2 \ , \end{aligned} \tag{C9}$$

where k' is the final wave number.

The corresponding cross section for charge exchange from the dominant second term of Eq. (C3) is

$$\begin{aligned} \sigma_{ce} &= \int d\Omega'' (2m/4\pi\hbar^2)^2 (k''/k) \left[\frac{1}{2j+1} \right] \\ &\quad \times \sum_{m,m'} \left| \sum_N \langle jjm, -m' | \lambda - N \rangle 2 C_{0j} C_{\lambda j} (T)^{-1/2} \hat{j} (\hat{\lambda})^{-1} \right. \\ &\qquad \left. \times \langle \chi_f(\hat{r}_0) | \mathcal{Y}_{\lambda,-N}(\hat{r}_0) \langle \lambda T_c T_c \| Q_{\lambda,10}(c) | | 0 T_c T_c \rangle | \chi_i(\hat{r}_0) \rangle \right|^2 \\ &= \int d\Omega'' (2m/4\pi\hbar^2)^2 (k''/k) 4 C_{0j}^2 C_{\lambda j}^2 (T)^{-1} (\hat{\lambda})^{-2} \\ &\quad \times \sum_N | \langle \chi_f(\hat{r}_0) | \mathcal{Y}_{\lambda,-N}(\hat{r}_0) \langle \lambda T_c T_c \| Q_{\lambda,10}(c) \| 0 T_c T_c \rangle | \chi_i(\hat{r}_0) \rangle |^2 \ . \end{aligned} \tag{C10}$$

Note that, aside from numerical constants and a different excitation Q value for charge exchange, leading to a different final wave number k'', the cross sections [Eqs. (C9) and (C10)] are the same except that the operator in Eq. (C9) is isoscalar and in Eq. (C10) is isovector. These matrix elements of different operators can be related using Eq. (C6). The Q value will be more negative for charge exchange than inelastic scattering, which favors the latter, both because $k' > k''$, and because the DW matrix element will suffer from a larger momentum mismatch.

Thus, by comparison of Eqs. (C10) and (C9), using Eq. (C6), we may infer that the cross section ratio satisfies the inequality

$$\frac{\sigma_{ce}}{\sigma_{in}} \approx 4 C_{0j}^2 C_{\lambda j}^2 (T)^{-1} \left[\frac{\beta_1 V_1}{\beta_0 V_0} \frac{N-Z}{A} \right]^2 \leq (T)^{-1} \left[\frac{\beta_1 V_1}{\beta_0 V_0} \frac{N-Z}{A} \right]^2 , \tag{C11}$$

the last inequality following because the upper limit on the mixing coefficient product $C_{0j} C_{\lambda j}$ is $\frac{1}{2}$.

[1] V. A. Madsen, V. R. Brown, S. M. Grimes, C. H. Poppe, J. D. Anderson, J. C. Davis, and C. Wong, Phys. Rev. C **13**, 548 (1976).
[2] J. D. Anderson, R. W. Bauer, V. R. Brown, S. M. Grimes, V. A. Madsen, B. A. Pohl, C. H. Poppe, and W. Scobel, Phys. Rev. C **38**, 1601 (1988).
[3] J. D. Anderson, V. R. Brown, R. W. Bauer, B. A. Pohl, C. H. Poppe, S. Stamer, E. Mordhorst, W. Scobel, S. M. Grimes, and V. A. Madsen, Phys. Rev. C **41**, 1993 (1990).
[4] A. M. Lane, Phys. Rev. Lett. **8**, 171 (1962); Nucl. Phys. **35**, 676 (1962).
[5] C. H. Poppe, S. M. Grimes, J. D. Anderson, J. C. Davis, W. H. Dunlop, and C. Wong, Phys. Rev. Lett. **33**, 856 (1974).
[6] S. M. Grimes, C. H. Poppe, J. D. Anderson, J. C. Davis, W. H. Dunlop, and C. Wong, Phys. Rev. C **11**, 158 (1975).
[7] C. D. Goodman, J. D. Anderson, and C. Wong, Phys. Rev. **156**, 1249 (1967).
[8] V. R. Brown, C. Wong, C. H. Poppe, J. D. Anderson, J. C. Davis, S. M. Grimes, and V. A. Madsen, Phys. Rev. C **33**, 1235 (1986).
[9] V. A. Madsen and M. J. Stomp (unpublished).
[10] J. D. Anderson, in *Isobaric Spin in Nuclear Physics,* edited by J. D. Fox and D. Robson (Academic, New York, 1966), p. 530.
[11] Y. Holler, A. Kaminsky, B. Scharlemann, H. Krause, R. Langkau, W. Peters, G. Poppe, N. Schirm, W. Scobel, and R. Wien, Nucl. Instrum. Methods A **235**, 123 (1985).
[12] E. Mordhorst, M. Trabandt, A. Kaminsky, H. Krause, and W. Scobel, Phys. Rev. C **34**, 103 (1986).
[13] W. Stoeffl (private communication).
[14] H. H. Bolotin and D. A. McClure, Phys. Rev. C **3**, 797 (1971).
[15] D. De Frenne, E. Jacobs, M. Verboven, and P. De Gelder, Nucl. Data Sheets **47**, 261 (1986). See also J. S. Geiger, R. L. Graham, and D. Ward, Atomic Energy of Canada Ltd. Report No. AECL-3667, 1970, p. 43.
[16] J. D. McCullen, B. Bayman, and L. Zamick, Phys. Rev. **134**, B515 (1964).
[17] M. A. Preston, *Physics of the Nucleus* (Addison-Wesley, Reading, MA, 1962), Chap. 4.
[18] A. M. Lane, *Nuclear Theory* (Benjamin, New York, 1964), p. 21.
[19] V. R. Brown and V. A. Madsen, Phys. Rev. C **11**, 1298 (1975).
[20] F. Petrovich, H. McManus, V. A. Madsen, and J. Atkinson, Phys. Rev. Lett. **22**, 895 (1968). The ratio $V_1/V_0=\frac{1}{2}$ can also be deduced from optical potentials in this energy range, for which $V_T\approx 100$ MeV, $V_0\approx 50$ MeV, taking into account the factor of 2 between the isospin operators τ and t.
[21] V. Riech, E. Fretwurst, G. Lindstroem, K. F. Von Reden, R. Schwerwinski, and H. P. Blok, Phys. Lett. B **178**, 10 (1986).
[22] V. A. Madsen, M. J. Stomp, V. R. Brown, J. D. Anderson, L. Hansen, C. Wong, and J. J. Wesolowski, Phys. Rev. Lett. **28**, 629 (1972).
[23] V. A. Madsen and V. R. Brown, in *The (p,n) Reaction and the Nucleon Nucleon Force,* edited by C. D. Goodman, S. M. Austin, S. D. Bloom, J. Rapaport, and G. R. Satchler (Plenum, New York, 1980), p. 433.
[24] C. Mahaux and H. Ngo, Nucl. Phys. **A378**, 205 (1982).
[25] C. Wong, J. D. Anderson, J. C. Davis, and S. M. Grimes, Phys. Rev. C **7**, 1895 (1973).
[26] V. A. Madsen, Nucl. Phys. **80**, 177 (1966); in *Nuclear Spectroscopy and Reactions,* edited by J. Cerny (Academic, New York, 1975), p. 260.
[27] G. R. Satchler, R. M. Drisko, and R. H. Bassel, Phys. Rev. **136**, B637 (1964).
[28] V. A. Madsen, V. R. Brown, and J. D. Anderson, Phys. Rev. C **12**, 1205 (1975).